



TITLE:

Limits in the High Resolution Electron Microscopy of Halogen Substituted Organic Molecule Single Crystals Caused by Radiation Damage (Commemoration Issue Dedicated to Professor Eiji Suito on the Occasion of his Retirement)

AUTHOR(S):

Kobayashi, Takashi; Reimwe, Kudwig

CITATION:

Kobayashi, Takashi ...[et al]. Limits in the High Resolution Electron Microscopy of Halogen Substituted Organic Molecule Single Crystals Caused by Radiation Damage (Commemoration Issue Dedicated to Professor Eiji Suito on the Occasion of his Retirement). Bulletin of the Institute for Chemical Research, Kyoto University 1975, 53(2): 105-116

ISSUE DATE:

1975-09-25

URL:

<http://hdl.handle.net/2433/76613>

RIGHT:

Limits in the High Resolution Electron Microscopy of Halogen Substituted Organic Molecule Single Crystals Caused by Radiation Damage

Takashi KOBAYASHI* and Ludwig REIMER**

Received March 3, 1975

The decrease of the reflection intensities in electron diffraction diagrams of tetrabromoquinone, hexabromobenzene and hexadecachloro-copper-phthalocyanine single crystal films was used to obtain a quantitative measure of radiation damage. The films were obtained by epitaxial growth on KCl and NaCl cleavage planes. Two different methods were used for recording the integral reflection spot intensity. The first records the intensity of a diffraction diagram directly by a scanning method. The second employs photometry of a photographic plate with a rectangular spread of the spot, produced by a small scanning amplitude during the exposure. The electron diffraction spots disappear at charge densities (end point doses) in the specimen plane of 15–40 C.cm⁻² for hexadecachloro-copper-phthalocyanine, 2.0–2.9 C.cm⁻² for hexabromobenzene and 0.19–0.20 C.cm⁻² for tetrabromoquinone. The consequences for the imaging of lattice structures are discussed. There are differences in the damage dose for different reflections. The displacements \bar{u}^2 are calculated by a Debye-Waller factor, but this value varies strongly for different reflections and decreases with increasing reciprocal lattice vector g , whereas for pure statistical displacements of the atoms there should be no dependence on g .

INTRODUCTION

Photographic emulsions used in electron microscopy need an incident charge density at 100 keV in the order of 10⁻¹¹ C.cm⁻² to give an exposure with an optical density $S=1$. High resolution requires a magnification in the order of $2-5 \times 10^5$. That means one has to operate at 100 keV with charge densities of 0.4–2.5 C.cm⁻² in the specimen plane which is equivalent to 250–1500 incident electrons on an area of 1 Å². 1 C.cm⁻² corresponds to an irradiation dose of 4×10^{11} rad¹⁹⁾ or 25 eV.Å⁻³. This high electron density causes ruptures of chemical bonds and results in a loss of a large fraction of H, O, and N atoms. Also some carbon atoms can leave the specimen as split radicals. The first process is an excitation of an electronic state in the molecule. This can result in a bond rupture, but the excitation energy can also be spread over a larger part of the molecule, so that at no part of the molecule is the energy for the rupture of a bond available. The latter possibility is especially true for aromatic compounds with the special electronic resonance structure of the benzene ring.¹³⁾ Aromatic compounds, therefore, show a resistance one order of magnitude higher than aliphatic ones.¹⁻³⁾ Another possibility of increasing the resistance is the substitution of hydrogen by halogen atoms.⁴⁾ As a

* 小林隆史: Laboratory of Crystal and Powder Chemistry, Institute for Chemical Research, Kyoto University, Uji, Kyoto.

** Present address: Physikalisches Institut der Universität Münster, Elektronenmikroskopische Abteilung, 44 Münster, West-Germany.

result a high resolution of the lattice structure is obtainable for Cl substituted Cu phthalocyanine single crystal films.^{5,6)}

One of the methods of measuring the radiation damage by a change in a physical property is the observation of the decrease of reflection intensities in electron diffraction diagrams.¹⁾ The diffraction diagram corresponds to a Fourier transform of a projected crystal potential. The image amplitude is obtained by an inverse Fourier transform after multiplying the diffracted amplitudes by a phase factor caused by the spherical aberration constant of the objective lens and by defocusing. Therefore, one can observe an image of the projection of the crystal unit cell as long as one has enough intensity in the diffraction spots. This method of electron diffraction for the investigation of radiation damage is, therefore, not only the easiest one within the electron microscope but has also a direct practical application.

Some work has been reported on polycrystalline evaporated films of organic material.^{1,2,7,8)} The resulting Debye-Scherrer rings have the advantage of being easily recorded with a photometer or by direct scanning of the diffraction diagram over a slit on top of an electron detector. One can irradiate large areas of the specimen (about $100 \times 100 \mu\text{m}$) and therefore work with a low current density in the specimen plane. Other investigations used single crystal films and selected area diffraction.^{4,9-12)} Selected area diffraction needs a higher current density and can, therefore, be used for the investigation of material with high radiation resistance. In single crystal diagrams one can also measure the decrease of intensity for high order reflections, whereas in polycrystalline films only Debye-Scherrer rings with low indices can be recorded.

EXPERIMENTAL

1. Methods of Measuring the Reflection Intensities

Two different methods were used for measuring the intensity of the diffraction spots. In both an electron diffraction pattern is produced on the viewing screen of a JEOL 100 B electron microscope by selected area diffraction on a crystal flake of the single crystal film. A pair of orthogonal scanning coils were mounted below the projection lens and powered by the amplified scan currents of the scanning attachment to the JEOL 100 B. In the first method the diffraction diagrams scans over a diaphragm of $750 \mu\text{m}$ diameter on top of the electron detector for transmitted electrons. The recorded aperture is of the order of a spot diameter. Therefore, the video signal of the detector is proportional to the integral intensity, if the spot scans over the centre of the aperture. The trace on the screen of an oscillograph is photographed with the Y-modulation technique (Fig. 5). Such a diagram normally shows high brightness in the background and lower in the peaks caused by the diffraction spots, because of the higher speed of the recording beam. Therefore, we have used reduced brightness of the recording beam in the background and switched to a higher brightness by changing the Wehnelt voltage of the oscillograph when the video signal shows a higher derivative inside the spots. This electronic switching technique offers the possibility for measuring the integral spot intensity by the height of the Y-modulation peaks. One Y-modulation image can be recorded in 50 s and the specimen is loaded with a charge density of about $1\text{--}2 \text{ C}\cdot\text{cm}^{-2}$. Therefore, this technique is especially applicable to substance with high radiation resistance

and one can take several Y-modulation images during the whole dose for complete damage.

In the second method the diagram is recorded on a photographic plate and the diffraction spots were broadened to rectangles by smaller currents in the scanning coils. A photometer record gives the integral spot intensity and one has no difficulty in finding the centre of the spot. Furthermore, one has no overexposure in the spot centres.

2. Preparation of the Single Crystal Films

a) *Tetrabromoquinone* ($C_6Br_4O_2$) (*bromanil*)

This substance was vacuum condensed on a cleaved KCl single crystal surface at room temperature. The film thickness of about 500 Å was measured with a quartz thickness monitor. The orientation of the film is in accordance with the reported result of Neuhaus.¹⁸⁾ The selected area diffraction pattern from this film (Fig. 1) shows that the film grows in the a-b plane. The unit cell dimensions¹⁵⁾ of this crystal are $a=8.62$ Å, $b=6.17$ Å, $c=9.03$ Å and $\beta=74.2^\circ$.

b) *Hexabromobenzene* (C_6Br_6)

The epitaxial growth condition of this material has not been reported. According to the surface treatment of the freshly cleaved (001) face of KCl and NaCl single crystals, three different orientations can be obtained. Although this material has two different polymorphs, the selected area diffraction pattern shows that the vacuum condensed film has unit cell dimensions of $a=8.40$ Å, $b=4.01$ Å, $c=17.14$ Å and $\beta=116.3^\circ$. This is the isomorphic structure of hexachlorobenzene (C_6Cl_6), if the space group of C_6Cl_6 is taken as $P2_1/c$, whose structure was reported by Brown and Strydom.¹⁶⁾ The molecule is stacked in the crystal b-axis and the molecule plane makes an angle of 23° with the a-c plane. If the (001) plane of a KCl or NaCl substrate is not preheated in vacuum,

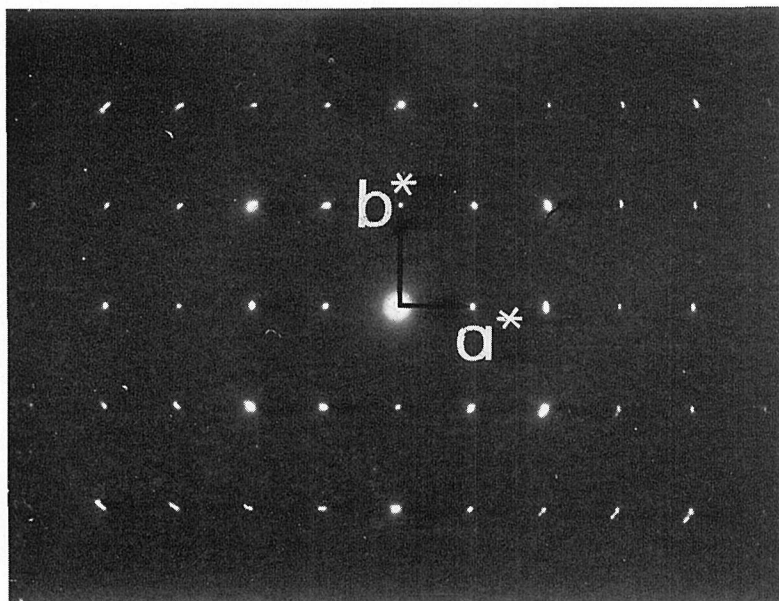


Fig. 1. Diffraction diagram of tetrabromoquinone on preheated KCl cleavage plane with the substrate at room temperature during deposition.

two directionally elongated crystals can be obtained. The fibre axis is revealed to the b-axis and another direction perpendicular to the axis is the c-axis or $10\bar{2}$ -axis as shown by electron diffraction in Fig. 2a and 2b. In the present work these two different orientations were used to measure the effect of crystal anisotropy on the damage rates.

On the preheated substrate the crystal grows with another orientation. The diffraction patterns (Fig. 3a) indicate that the crystal axis is inclined to the substrate plane similar to metal-phthalocyanine crystals deposited on a preheated surface of alkali halides or muscovite.¹⁷⁾ When this film is inclined at about 25° to the incident beam with the aid of a universal goniometer stage, it gives the diffraction pattern of a a^*c^* plane (Fig. 3b). This fact indicates that in this case the molecular plane of the hexabromobenzene is parallel to the substrate surface. This orientation is not adequate for the present purpose.

c) *Hexadecachloro-copper-phthalocyanine*

The crystal growth of this substance on the (001) plane of KCl was reported elsewhere⁵⁾. On the surface, which was baked in vacuum at about 400°C for one hour, the crystals grow as thin rhombic platelets at about 400°C and the crystal c^* -axis is perpendicular to the substrate surface. The crystal data reported are $a=19.6\text{ \AA}$, $b=26.0\text{ \AA}$, $c=3.68\text{ \AA}$ and $\beta=116.5^\circ$. If this crystal is inclined about the b-axis a a^*b^* plane diffraction pattern is obtained. The first described technique for measuring the reflection intensities is adequate for the initial diffraction pattern (Figs. 4a and 5) and the second one is better for the a^*b^* plane (Fig. 4b) because of the short distances between the diffraction spots.

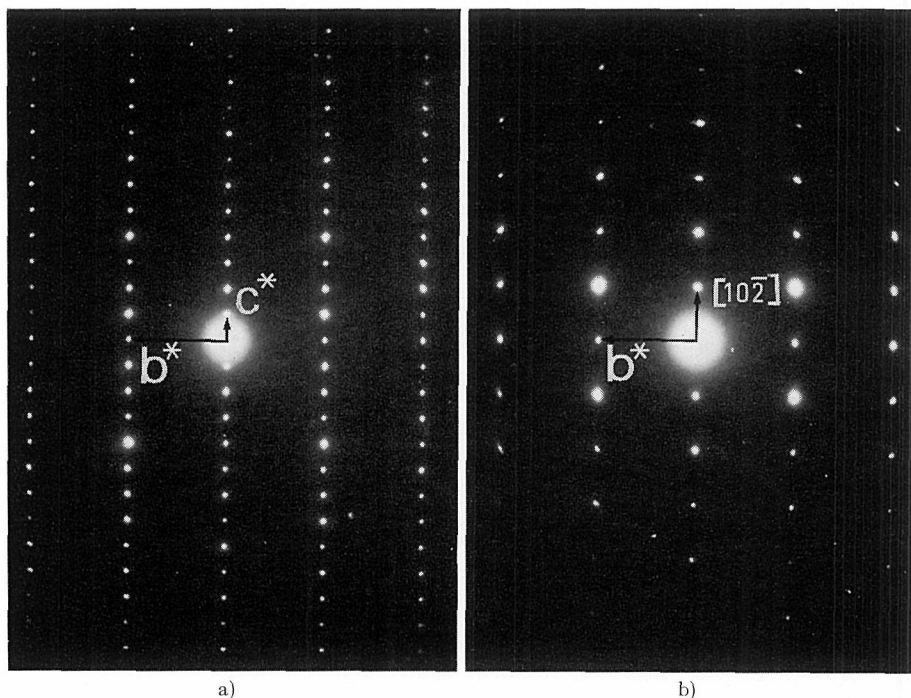


Fig. 2. Diffraction diagram of hexabromobenzene on unheated KCl cleavage plane in two different orientations a) and b).

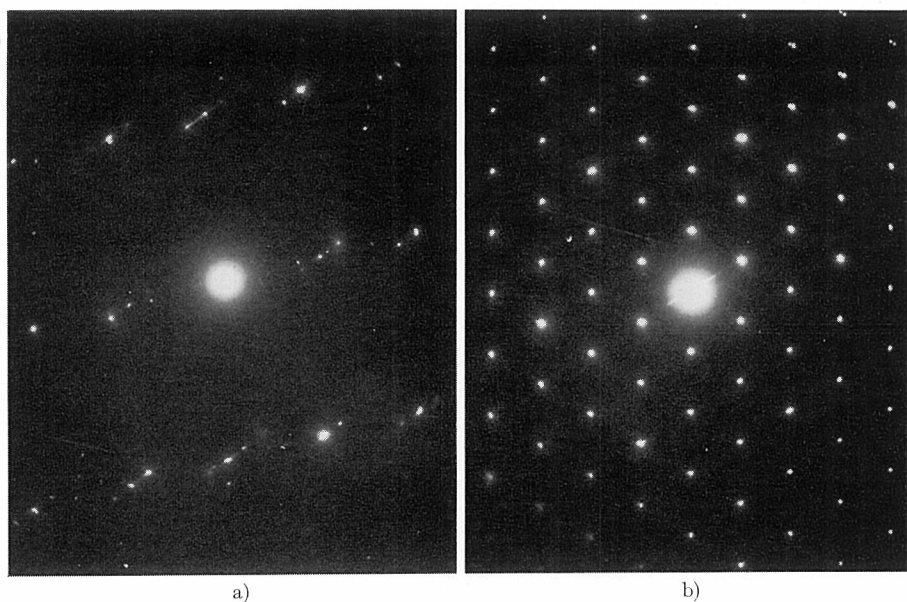


Fig. 3. Diffraction diagram of hexabromobenzene on preheated KCl cleavage plane with the normal of the film a) parallel and b) inclined 23° to the electron beam.

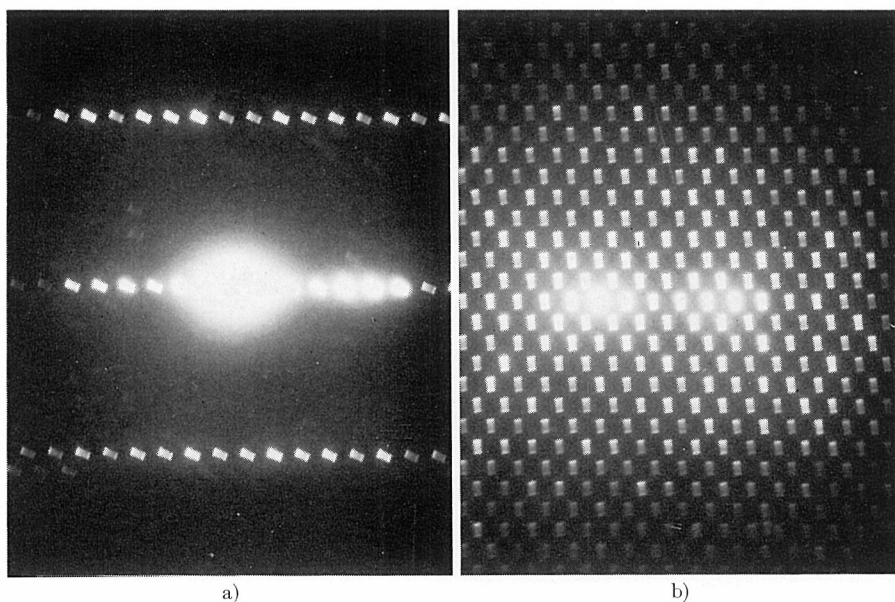


Fig. 4. Diffraction diagram of hexadecachloro-copper-phthalocyanine on a KCl cleavage plane at a substrate temperature of 400°C with the normal of the film a) parallel, b) inclined 25° to the electron beam. Bragg reflection spots were broadened by scanning the diagram during the exposure of the photographic emulsion.

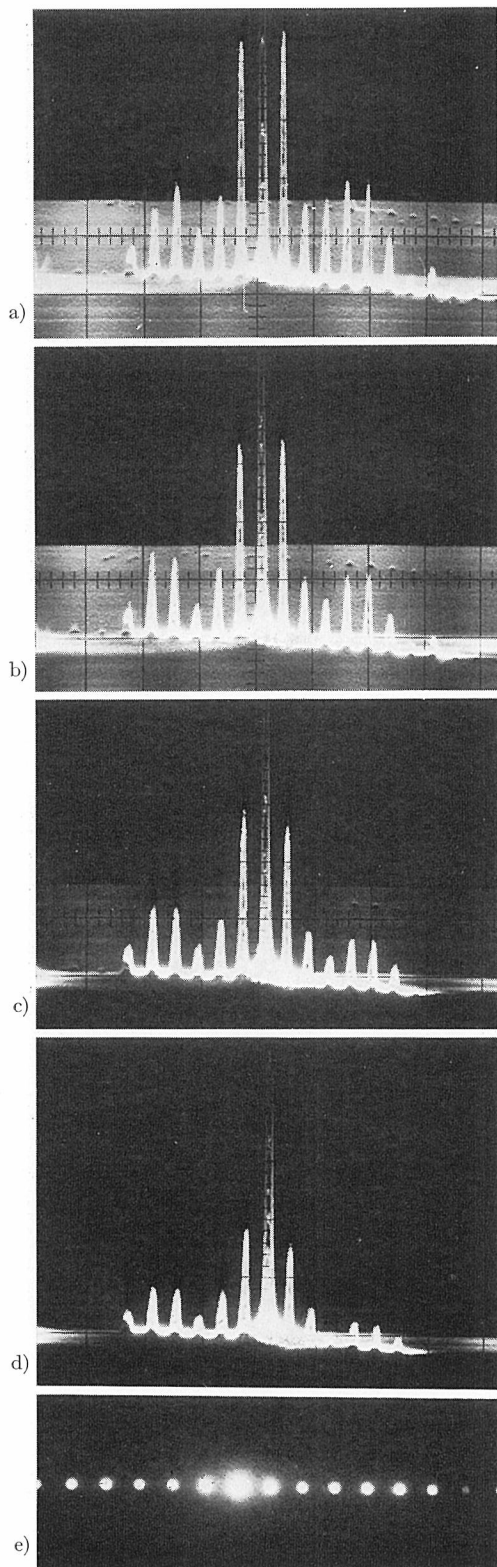


Fig. 5. Demonstration of the decrease of integral intensity of the diffraction spots in the diffraction diagram (e) of a hexadecachloro-copper-phthalocyanine film $[(0k0)\text{-row}, k=2n]$ obtained by direct scanning of the diagram and recording with the Y-modulation technique. Current density in the specimen plane: $3 \times 10^{-2} \text{ A.cm}^{-2}$; start of recording time after a) 0, b) 200 s, c) 350 s, d) 700 s of the irradiation.

RESULTS AND DISCUSSION

1. The End Point Dose for Total Damage

The ratios of the damage reduced to the initial intensities I/I_0 were plotted as a function of electron doses in $\text{C}\cdot\text{cm}^{-2}$ (Figs. 6–8). The end point dose is that radiation dose required to make this ratio zero and is obtained by extrapolation of this curve. Figure 5 demonstrates the intensity change of the $(0k0)$ systematic row of hexadecachloro-

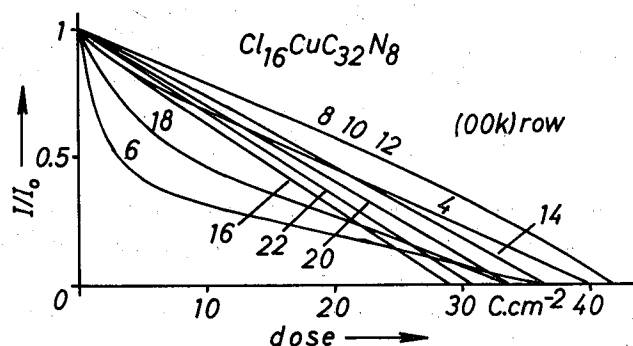


Fig. 6. Decrease of the relative integral intensity I/I_0 of diffraction spots of hexadecachloro-copper-phthalocyanine films as a function of irradiation dose.

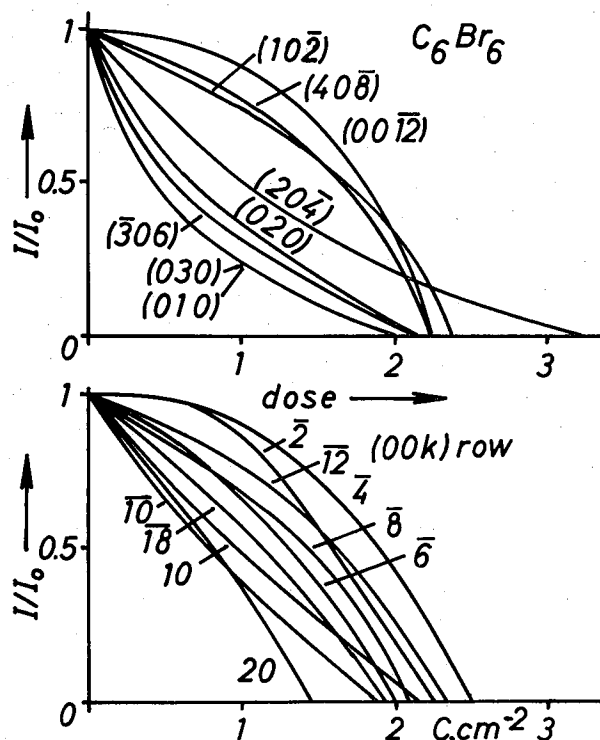


Fig. 7. As Fig. 6 for hexabromobenzene films.

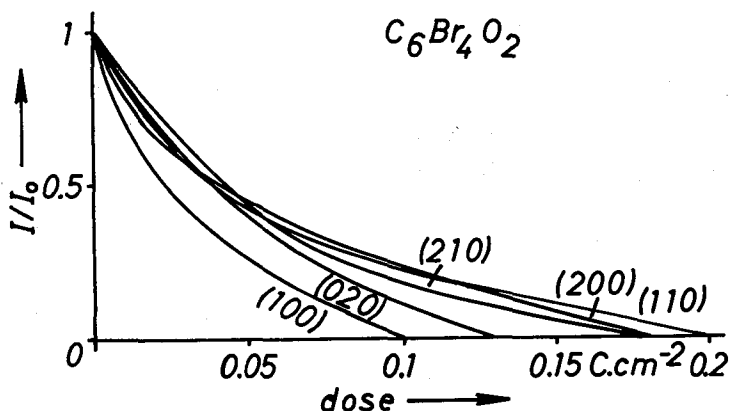


Fig. 8. As Fig. 6 for tetrabromoquinone films.

copper-phthalocyanine obtained by the first experimental method. The end point doses for each reflection of $(0k0)$ ($k=2n$) are $32 \pm 5 \text{ C}\cdot\text{cm}^{-2}$ in agreement with literature.⁴⁾ The same systematic row was also examined with the second method of photographic recording (Figs. 4a and 6). The end point dose for the $(0k0)$ row has an averaged value of $34 \pm 4 \text{ C}\cdot\text{cm}^{-2}$ but the first layer lines $(7k1)$ show a dose of $40 \pm 6 \text{ C}\cdot\text{cm}^{-2}$. A diffraction pattern of the a^*-c^* plane also gave a value of $33 \pm 5 \text{ C}\cdot\text{cm}^{-2}$ for a $(0k0)$ row. However, for the $(h00)$ row the end point doses change with h and values of 31 for (200), 37 for (400) 21 for (800) and $(10\ 0\ 0)$ and $15 \text{ C}\cdot\text{cm}^{-2}$ for $(12\ 0\ 0)$ are obtained.

The change of reflection intensities from hexabromobenzene are shown in Fig. 7. From the diffraction pattern of Fig. 2b the averaged end point dose of $2.4 \pm 0.5 \text{ C}\cdot\text{cm}^{-2}$ for the $(10\bar{2})$ systematic row and 2.0 ± 0.1 for (010) were obtained (Fig. 7a). Using a b - c plane diffraction diagram (Fig. 2a) the end point dose are 2.2 ± 0.3 for (001) and 2.0 ± 0.3 for (010). The space group of the crystal is $P2_1/c$ and therefore the (001) reflections with $l=2n-1$ are forbidden, although in the pattern of Fig. 2a they are clearly observed. Only the intensities with $l=2n$ were measured and averaged. The diffraction spots of $(20\bar{4})$ and $(11\bar{2})$ are the most stable and the end point dose of $2.9 \text{ C}\cdot\text{cm}^{-2}$ of $(20\bar{4})$ is the largest in the $(10\bar{2})$ systematic row. The intensities of four equivalent $(11\bar{2})$ planes are too strong to measure and a total dose larger than $5 \text{ C}\cdot\text{cm}^{-2}$ is needed for disappearance of the spots. The interplanar distances of these planes are 3.60 and 3.50 Å. It is of interest that the intermolecular and intramolecular distances in C_6Cl_6 crystal are 3.52 and 3.11 Å respectively and the ionic radii of Br and Cl are 1.95 and 1.81 Å. Therefore, the lattice distances of 3.60 and 3.50 Å are assumed to correspond to the Br-Br distance of this crystal.

In the case of tetrabromoquinone (210), (110), and (200) reflections are also stable (Fig. 8). These diffractions can be observed as diffuse spots even if all other spots have disappeared. The end point doses of tetrabromoquinone are $0.18 \pm 0.02 \text{ C}\cdot\text{cm}^{-2}$ for (200) and (210) and 0.20 ± 0.02 for (110). These values are averaged over two or four equivalent planes. Compared with the end point doses of hexabromobenzene the substitution of two opposite Br atoms by O atoms causes a decrease of radiation resistance of one order of magnitude.

Uyeda *et al.*²⁰⁾ succeeded in resolving the 4.1 Å lattice planes in tetrabromoquinone

single crystal films at 100 keV. If the above end point dose of $0.2 \text{ C}\cdot\text{cm}^{-2}$ for the low order reflections are compared with the necessary dose for the exposure of a photographic emulsion mentioned in the introduction of this paper, this resolution is seen to be just the limit resulting from the damage rates. Hexabromobenzene shows one order of magnitude higher radiation damage resistance even for high order reflections. It will be possible for this substance to resolve the projection of unit cells with the same resolution as in the hexadecachloro-copper-phthalocyanine crystals. The latter show a very high radiation resistance. Therefore, one can preirradiate these crystals for a longer time and look for a suitable orientation by tilting the specimen in a goniometer stage.

2. Discussion of the Decrease of Intensity of the Diffraction Spots

The decrease of intensity is caused by a crystal disorder. The damage will cause a statistical disorder and there are two main types of disordering, the displacement and substitution disorder. Both disorders decrease the intensity of the diffraction spots and increase the diffuse background. Depending on the nature of the disorder the intensity can be spread either completely diffusely or in more concentrated streaks between reflections, or in diffuse spots around the reflections. In the displacement disorder, the position of the atoms show a statistical deviation u from its ideal crystal position. A typical example is the displacement disorder by thermal vibrations. If independent vibrations of the atoms are assumed, the scattering is completely diffuse. With a phonon model one has for each phonon of the spectrum a long range periodicity of the displacements. This leads to a concentration of diffuse scattering in the vicinity of the diffraction spots. The decrease of the intensity in the diffraction spots can be described by the Debye-Waller factor

$$I=I_0 \exp(-4\pi^2 \overline{u^2} g^2) \quad (1)$$

with the root mean square (r.m.s.) of the atomic displacements u . This formula, however, only valid for the thermal vibrations of cubic monoatomic crystals. It is an important result, that this kind of disorder causes an increasing reduction of intensity with increasing reciprocal lattice vector g .

The substitution disorder shows perfect periodicity of the crystal but statistical variations of the structure amplitude of the unit cells. A typical example is a disordered solid solution in which two kinds of atoms are randomly distributed on lattice sites. The decrease of intensity is caused by a decrease of the mean structure amplitude only.

Further the diffraction spots can be influenced by a change of the lattice constant resulting in a spot shift, or by a decrease of the size of coherent scattering volume, resulting in a broadening of the diffraction spots (particle size effect). But no significant shifting or broadening was observed in this case.

If displacement disorder is dominant, one can determine the r.m.s. value of u by formula (1) as a disorder parameter with the dimension of a length, giving an order of magnitude of the displacements of single molecules. The factor g^2 in formula (1) should give the result that a reflection at a high Bragg angle is more sensitive than one at low angle. In addition all reflections of a systematic row, for example all of the (001) reflections, result in the same value of the r.m.s. of u at a damaged state. This is because the reduction of intensity by radiation damage should be produced only by the increase of $\overline{u^2}$.

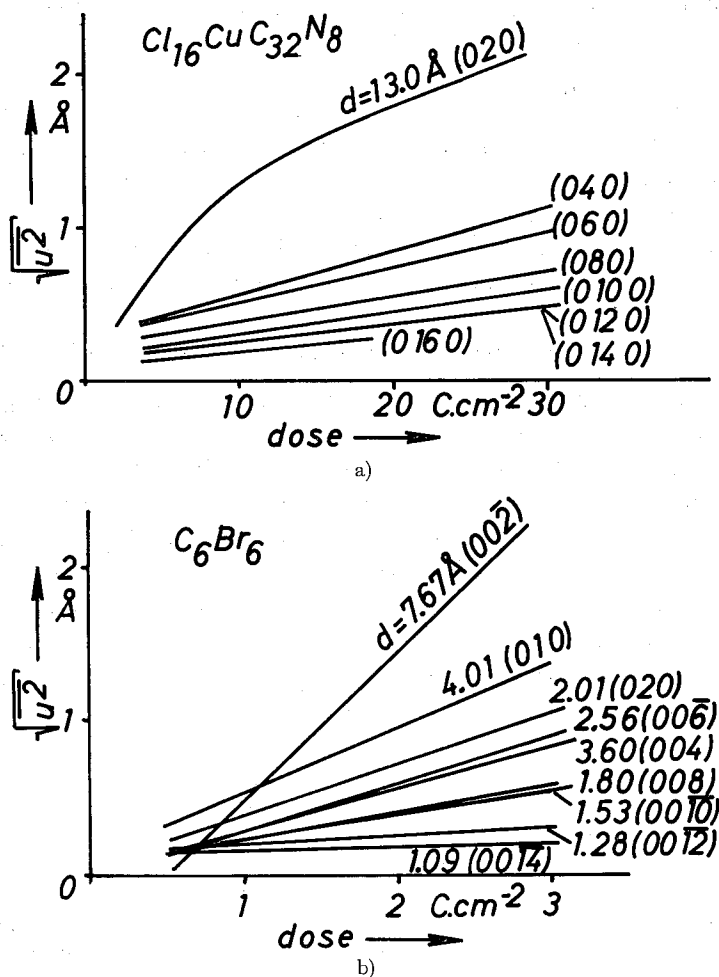


Fig. 9. The root mean square of the displacement u obtained from the Debye-Waller factor as a function of irradiation dose with I/I_0 values of a) hexadecachloro-copper-phthalocyanine from Fig. 5 (direct scanning method) and b) hexabromobenzene from Fig. 7.

Figures 9 and 10 show plots of the r.m.s. of u as a function of the radiation dose for systematic rows of hexadecachloro-copper-phthalocyanine and hexabromobenzene. One sees that the r.m.s. of u does not have a constant value but decreases with increasing g therefore, a kind of substitution disorder may be a better model for a damaged crystal. Because there is no detectable shift and broadening of the reflections one can assume that the long range order is conserved, but that with increasing damage an increased number of unit cells is damaged resulting in a lower value of the mean structure amplitude. But with increasing damage there are also the influences of statistical variations of lattice plane distances or diffraction spot broadening by small coherent volumes, because one observes an increase of anisotropic diffuse scattering near the spots and as streaks between the spots (Fig. 10). The intensity of this diffuse scattering is very low and small compared to the normal diffuse background. Therefore, it will be difficult to get further details

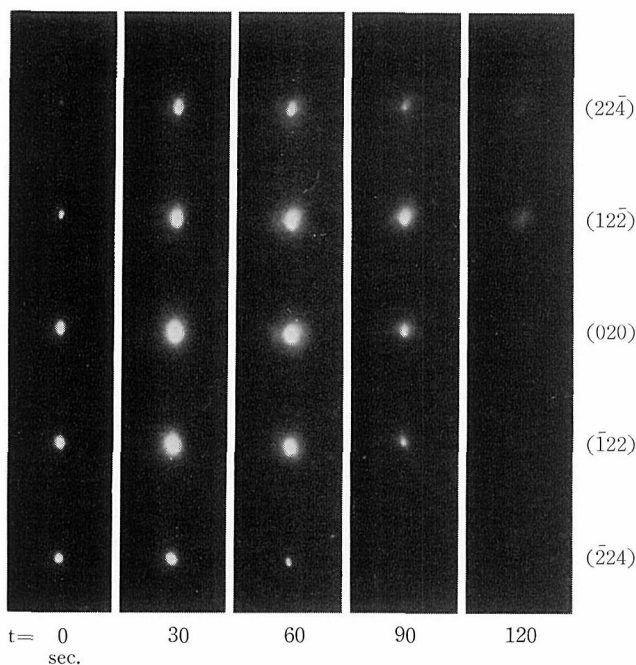


Fig. 10. The change of diffuse scattering in the (h21) row of hexabromobenzene with increasing irradiation dose. Current density in the specimen plane: 1.7×10^{-2} A.cm $^{-2}$; Irradiation time a) 0, b) 30 s, c) 60 s, d) 90 s and e) 120 s.

about the kind of damage from the diffuse scattering. But these experiments show that further measurements of the intensity in diffraction diagrams of single crystals together with other methods such as mass loss, optical absorption and energy losses will be a useful method to get information about the kinetic of the radiation damage at these high doses used in electron microscopy.

All experiments at higher voltages than 100 keV have shown that the damage decreases proportionally to v^{-2} because of the decreased ionisation rate in thin films. But there is only one extensive study by Siegel⁷⁾ of the decrease of damage at low specimen temperatures. To investigate the influence of temperature one needs rapid methods of measuring the diffraction spot intensities. The methods described in this paper offer this possibility.

ACKNOWLEDGMENTS

The authors thank Mr. P. Hagemann for the assistance in developing the experimental techniques. Thanks are also due to the Deutsche Forschungsgemeinschaft and the Alexander von Humboldt-Stiftung for financial support.

REFERENCES

- (1) L. Reimer, *Z. Naturforschung*, **15a**, 405 (1960).
- (2) L. Reimer, *Lab. Investigations*, **14**, 1082 (1965).

- (3) K. Stenn and G. F. Bahr, *J. Ultrastructure Res.*, **31**, 526 (1970).
- (4) N. Uyeda, T. Kobayashi, M. Ohara, M. Watanabe, T. Taoka, and Y. Harada, Proc. 5th Europ. Congr. Electron Microscopy, Institute of Physics, London, Bristol, 1972, p. 566.
- (5) N. Uyeda, T. Kobayashi, E. Suito, Y. Harada, and M. Watanabe, *Microscopie Electronique* 1970, Vol. I, 23; *J. Appl. Phys.*, **43**, 5181 (1972).
- (6) N. Uyeda, K. Ishizuka, Y. Saito, Y. Murata, K. Kobayashi and M. Ohara, *Electron Microscopy* 1974, Vol. I, 266.
- (7) G. Siegel, *Z. Naturforschung*, **27a**, 325 (1972).
- (8) T. Kobayashi, L. Reimer and J. Spruth, *Electron Microscopy* 1974, Vol. II, 682.
- (9) H. Kobayashi and K. Sakaoku, *Lab. Investigations*, **14**, 1097 (1965).
- (10) H. Orth and E. W. Fischer, *Z. Makromol. Chemie*, **88**, 188 (1965).
- (11) R. M. Glaeser, *J. Ultrastructure Res.*, **36**, 466 (1971).
- (12) D. T. Grubb and G. W. Groves, *Phil. Mag.*, **24**, 815 (1971).
- (13) W. J. Claffey and D. F. Parsons, *Phil. Mag.*, **25**, 637 (1972).
- (14) R. Spehr and H. Schnabl, *Z. Naturforschung*, **28a**, 1729 (1973).
- (15) I. Ueda, *J. Phys. Soc. Japan*, **16**, 1185 (1961).
- (16) G. M. Brown and O. A. W. Strydom, *Acta Cryst.*, **B30**, 801 (1974). 801
- (17) M. Ashida, *Bull. Chem. Soc. Japan*, **39**, 2625, 2632 (1966).
- (18) Landolt-Börnstein, New Series Group III, Vol. 8: Epitaxy Data of Inorganic and Organic Crystals, Berlin, Heidelberg, New York 1972.
- (19) W. Lippert, *Optik*, **15**, 293 (1958).
- (20) N. Uyeda, Y. Murata, and E. Suito, *Electron Microscopy* 1974, Vol. I, 692.